Int. J. Therm. Sci. (1999) 38, 854–862

Non-Darcy natural convection heat and mass transfer along a vertical permeable cylinder embedded in a porous medium

M. A. Hossain[a], Kambiz Vafai[b]*, Khalil M.N. Khanafer[b]

[a] *Department of Mathematics, University of Dhaka, Dhaka 1000, Bangladesh*
[b] *Department of Mechanical Engineering, Ohio State University, Ohio 43210-1107, USA*

(Received 12 December 1998, accepted 19 April 1999)

Abstract — Combined heat and mass transfer in non-Darcy natural convection flow along a permeable vertical cylinder embedded in a saturated porous medium is studied. The boundary layer analysis is formulated in terms of the combined thermal and solutal buoyancy effect. The flow field characteristics are analyzed using the implicit finite difference method as well as the local nonsimilarity method. The effect of the curvature, the buoyancy ratio, the Lewis number and the transpiration parameter on the local Nusselt number and the local Sherwood number are also studied. The results are presented in tabular form as well as graphically. Comparisons of the results obtained by the local nonsimilarity method are in excellent agreement with finite difference solution up to ξ (the curvature parameter) of 10. The effects of different pertinent parameters on the velocity, temperature and species concentration profiles are also shown graphically. ©1999 Éditions scientifiques et médicales Elsevier SAS.

porous media / natural convection / heat and mars transfer

Nomenclature

C	species concentration in the boundary layer
C_w	constant species concentration at the surface of the cylinder
C_∞	ambient constant species concentration
D	mass diffusivity
D_p	particle diameter
f	transformed stream function
f_w	blowing and suction parameter
g	acceleration due to gravity
Gr^*	modified Grashof number $g\beta_T K K^* (T_w - T_\infty)/\nu^2$
K	permeability of the porous media
K^*	Inertial coefficient defined in equation (5)
Le	Lewiss number defined in equation (18)
N	buoyancy ratio measures the effect of concentration buoyancy effect to the thermal buoyancy effect defined in equation (18)
Nu_x	local Nusselt number
r	radial coordinate
r_0	radius of the cylinder
Ra_x	modified local Rayleigh number defined in equation (11)
s	porosity
Sc	Schmidt number
Sh_x	local Sherwood number
T	temperature in the boundary layer
T_w	constant temperature at the surface of the cylinder
T_∞	ambient constant temperature particle diameter

* Correspondence and reprints.

u,V	reference velocity component in the x and r directions
V	surface mass flux
x	axial coordinate

Greek symbols

α	equivalent thermal diffusivity
β_T	thermal expansion coefficient
β_C	concentration expansion coefficient
ϕ	dimensionless concentration function
η	pseudosimilarity variable
ν	fluid kinematic viscosity
θ	dimensionless temperature function
ρ	density of the fluid
ξ	stretched streamwise coordinate
Ψ	stream function

1. INTRODUCTION

Natural convection heat and mass transfer driven by combined thermal and solutal buoyancy forces in a porous medium have received considerable attention in the past decades [1, 2]. This attention stems from its importance in many geophysical and engineering applications. Such applications include the movement of contaminants in ground water, moisture transport in thermal insulation, underground nuclear waste storage sites, and grain storage installations. Most of the investigations on heat and mass transfer flows driven by temperature and concentration variations are focused mainly on the convective instability of porous layers with imposed vertical temperature and concentration gradients [3–5]. Pera and Gebhart [6] and Chen et al. [7] studied the wave and vortex modes of the instability of a horizontal and inclined free convection under the combined buoyancy effects. The interaction between the two buoyancy effects that drive the flow in porous media, namely, the density difference caused by the concentration variations and the density difference caused by the temperature variations in porous media subjected to a horizontal density gradient have received less attention. Bejan and Khair [8] presented in their study a scale analysis of heat and mass transfer about a vertical plate embedded in a porous media. They considered concentration gradients, which aid or oppose thermal gradients, but reported limited similarity results for the latter case. Later on, Trevisan and Bejan [9] extended the analysis to a porous medium confined between two vertical walls maintained at different temperature and concentration levels. Rapits et al. [10] conducted a steady-state analysis on the effect of the natural convection flow and mass transfer on a viscous flow through a porous medium bounded by a vertical infinite plate. In this study, they considered a case when the temperature and the concentration on the plate are kept constant. Evan and Nunn [11] investigated free thermoheline convective in sediments surrounding a salt column.

The problem of free convection about a vertical cylinder in a porous medium due to combined driving forces has been studied by Yücel [12]. In this investigation, Yücel formulated the problem by considering the combined buoyancy effect rather than the limiting case of heat- or mass-transfer driven flow. In this analysis, the range of buoyancy parameters and the Lewis number for which flows are possible were identified for both favorable and adverse solute density gradients. A scale analysis originally suggested by Bejan [13] was introduced for four possible regimes depending on the buoyancy ratio and Lewis number, and numerical solutions to the boundary layer equations were obtained for a limited range of buoyancy ratios. Recently, Nakayama and Hossain [14] revisited the physical model of Bejan and Khair, and then extended it for the case of arbitrary shapes. Highly accurate heat and mass transfer formulae, which cover all ranges of the buoyancy ratio and Lewis number are obtained by using a simple integral treatment. All possible physical limiting conditions are examined to construct two distinct regime maps for heat transfer and mass transfer, respectively, which subsequently lead to an interesting paradox.

All the above studies were confined to the case of Darcy flow. Vafai and Tien [15] investigated the effects of a solid boundary and the inertial forces on flow and heat transfer in porous media. The results showed significant effects on the heat transfer rate with the introduction of the viscous effects due to frictional drag at the boundary and the inertial drag.

The problem of simultaneous heat and mass transfer accompanied by phase changes in porous insulation was investigated by Vafai and Whitaker [16]. In their study, they used the local volume-averaging technique to arrive at a rigorous and fundamental formulation of the heat and mass transfer process in an insulating material. Most of the recent studies on non-Darcy natural convection in porous media deal with the thermal driving force alone as done by Minkowycz and Cheng [17] for the natural convection flow about a vertical cylinder embedded in a saturated porous medium with variable surface temperature. Later investigations were performed by Vasanth et al. [18], for flow from an isotherm slender vertical frustum of a cone, Ingham [19], for the flow from a axisymmetric bodies of arbitrary shape and Hossain and Nakayama [20] for the flow along a vertical cylinder with surface mass flux. Very recently, the non-Darcian effects on double-diffusive convection flow within a porous medium have been investigated by Fard et al. [21].

The present study addresses the combined effect of heat and mass transfer on the natural convection flow of a non-Darcy fluid from a vertical permeable cylinder embedded in a porous medium. The governing equations are obtained in terms of local nonsimilarity equations. Numerical solutions are obtained by employing the method of local nonsimilarity and the implicit finite difference method for wide range of pertinent parameters, namely, the buoyancy ratio, N, the Lewis

number, Le, the modified Grashof number, Gr^*, and the transverse curvature parameter, ξ. Results obtained from this study will be helpful in predicting flow, heat transfer, and solute or concentration dispersion about intrusive bodies such as salt domes, magnetic intrusions, piping and easing system and similar structures found in these applications.

2. MATHEMATICAL FORMULATION

Consider the problem of steady non-Darcy free convection flow of a viscous incompressible fluid about a vertical porous cylinder of radius r_0 embedded in a saturated porous medium at temperature T and concentration C. The surface of the cylinder is maintained at a uniform temperature T_w and uniform concentration C_w. The physical model and the coordinate system are shown in *figure 1.*

In this investigation, the porous medium is assumed to be homogeneous and isotropic, The physical properties are assumed to be constant except for the density variation in the buoyancy term. The fluid and solid phases are in local thermal equilibrium since the flow is assumed to be sufficiently slow. Also, the analysis is confined to small concentration variations such that the cross diffusion effects and the interfacial velocity at the cylinder surface due to mass diffusion can be neglected. Under these assumptions, the boundary layer equations governing the flow, the energy and solute transport in cylindrical coordinates are

$$\frac{\partial}{\partial x}(r\,u) + \frac{\partial}{\partial r}(r\,\mathsf{V}) = 0 \tag{1}$$

$$u + \frac{K^*}{\nu}\,u^2 = \frac{g\,K}{\nu}\,[\beta_T\,(T - T_\infty) + \beta_C\,(C - C_\infty)] \tag{2}$$

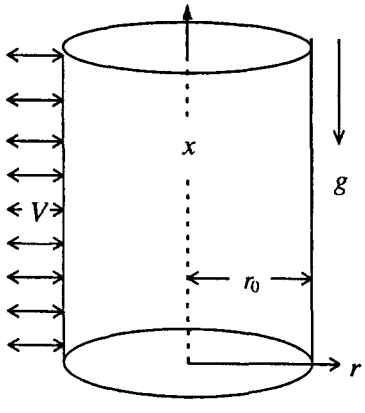

Figure 1. Physical model and the coordinate system.

$$u\,\frac{\partial T}{\partial x} + \mathsf{V}\,\frac{\partial T}{\partial r} = \frac{\alpha}{r}\,\frac{\partial}{\partial r}\left(r\,\frac{\partial T}{\partial r}\right) \tag{3}$$

$$u\,\frac{\partial C}{\partial x} + \mathsf{V}\,\frac{\partial C}{\partial r} = \frac{D}{r}\,\frac{\partial}{\partial r}\left(r\,\frac{\partial C}{\partial r}\right) \tag{4}$$

where, u, V, T and C are volume-averaged quantities representing respectively the velocity components in the x- and r-directions, ν is the kinetic coefficient of viscosity, g is the acceleration due to gravity, α and D are the equivalent thermal and mass diffusivities specially of the saturated porous medium, β_T and β_C are, respectively, the absolute values of the coefficient of thermal and concentration expansion. In equation (2), K and K^* are respectively the permeability and the inertial coefficients expressed in terms of characteristic pore or particle diameter D_p and porosity s. These are defined as given below:

$$K = \frac{D_p^2\,s^3}{150\,(1-s)^2} \quad \text{and} \quad K^* = \frac{1.75\,D_p}{150\,(1-s)} \tag{5}$$

Further, equation (2) approaches Darcy's law for very small K^*. According to Plumb and Huenfeld [22], the inertial effects are found to be significant when $g\beta K K^*(T_w - T_\infty)/\nu^2 > 0.1$.

The boundary conditions for the present problem are:

$$\left.\begin{aligned} r = r_0 &: \mathsf{V} = V(x),\ T = T_w,\ C = C_w \\ r \to \infty &: u = 0,\ T = T_\infty,\ C = C_\infty \end{aligned}\right\} \tag{6}$$

Near the leading edge, the flow is caused mainly by the effect of the buoyancy force, which arises from the difference in temperature between the plate and the ambient fluid. Therefore the following group of transformations are introduced in (2) and (3).

$$\Psi(x,y) = \alpha\,r_0\,Ra_x^{1/2}\,f(\xi,\eta) \tag{7}$$

$$T - T_\infty = (T_w - T_\infty)\,\theta(\xi,\eta) \tag{8}$$

$$C - C_\infty = (C_w - C_\infty)\,\phi(\xi,\eta) \tag{9}$$

where Ψ is the stream function satisfying the equation of continuity (1), and

$$\eta = \frac{Ra_x^{1/2}}{2\,r_0\,x}\,\left(r^2 - r_0^2\right), \quad \xi = \frac{2\,x}{r_0}\,Ra_x^{-1/2},$$
$$V(x) = V_0\,x^{-1/2} \tag{10}$$

where

$$Ra_x = g\,K\,[\beta_T\,(T_w - T_\infty) + \beta_C\,(C_w - C_\infty)]\,x/\alpha\,\nu \tag{11}$$

is the modified local Rayleigh number for a saturated porous medium, and is defined to represent the

combined buoyant driving force and the stream function Ψ is defined by

$$r\,u = \frac{\partial \Psi}{\partial r}, \quad r\,\mathrm{V} = -\frac{\partial \Psi}{\partial x} \tag{12}$$

which satisfies the equation of continuity (1). Introducing the variables defined above into (10), we have

$$r\,u = \frac{\alpha}{x}\, Ra_x^{1/2}\, f'(\xi,\eta) \tag{13}$$

and

$$r\,\mathrm{V} = \frac{\alpha\, r_0}{2\,r\,x} Ra_x^{1/2}\, \left\{(\eta\, f' - \xi\, f_\xi) - f\right\} \tag{14}$$

Equations (1–3) now become:

$$f'' + 2\, Gr^*\, (1+N)\, f'\, f'' = \frac{\theta' + N\phi'}{1+N} \tag{15}$$

$$(1+\xi\,\eta)\,\theta'' + \frac{1}{2}\,(f+\xi)\,\theta' = \frac{1}{2}\,\xi\left(f'\,\frac{\partial\theta}{\partial\xi} - \theta'\,\frac{\partial f}{\partial\xi}\right) \tag{16}$$

$$\frac{1}{Le}\,(1+\xi\,\eta)\,\phi'' + \frac{1}{2}\,(f+\xi)\,\phi' = \frac{1}{2}\,\xi\left(f'\,\frac{\partial\phi}{\partial\xi} - \phi'\,\frac{\partial f}{\partial\xi}\right) \tag{17}$$

where primes denote differentiation with respect to η and

$$Gr^* = \frac{g\,\beta_T\, K\, K^*\,(T_\mathrm{w} - T_\infty)}{\nu^2}$$

$$Le = \frac{\alpha}{D} = \frac{Sc}{Pr} \quad \text{and} \quad N = \frac{\beta_C\,(C_\mathrm{w} - C_\infty)}{\beta_T\,(T_\mathrm{w} - T_\infty)} \tag{18}$$

are, respectively, the modified local Grashof number expressing the relative importance of the inertial effects, the Lewis number and the buoyancy ratio that measures the ratio of the concentration buoyancy effect to thermal buoyancy effect.

The corresponding boundary conditions transform into

$$\left.\begin{aligned} f &= f_\mathrm{w},\, \theta = 1,\, \phi = 1 \;\text{ at }\; \eta = 0 \\ f' &= 0,\, \theta = 0,\, \phi = 0 \;\text{ as }\; \eta \to \infty \end{aligned}\right\} \tag{19}$$

where $f_\mathrm{w}(= -2\,V_0/\alpha)$ is the dimensionless transpiration parameter, which is positive for suction and negative for blowing of fluid through the surface of the cylinder. It is also necessary to note that $N = 0$ for no species diffusion, $N \to \infty$ for no thermal diffusion, $N > 0$ for both effects combining to drive the flow and $N < 0$ for the opposite effects.

For the flow adjacent to the surface of the cylinder, the local rate of heat transfer and the local chemical species transfer which may be obtained in terms of local Nusselt number Nu_x and local Sherwood number Sh_x from the following relations:

$$Nu_x = -Ra_x^{1/2}\,\theta'(\xi,0) = -Ra_{x,t}^{1/2}\,(1+N)\,\theta'(\xi,0) \tag{20}$$

and

$$Sh_x = -Ra_x^{1/2}\,\phi'(\xi,0) = -Ra_{x,c}^{1/2}\,\left|\frac{1+N}{N}\right|^{1/2}\,\phi'(\xi,0) \tag{21}$$

In equations (20) and (21), the parameters $Ra_{x,T}$ and $Ra_{x,C}$ are defined as

$$Ra_{x,T} = \frac{g\,K\,\beta_T\,(T_\mathrm{w} - T_\infty)\,x}{\alpha\,\nu} \tag{22}$$

and

$$Ra_{x,C} = \frac{g\,K\,\beta_C\,(C_\mathrm{w} - C_\infty)\,x}{\alpha\,\nu} \tag{23}$$

It is to be noted that the absolute value in equation (21) is necessary since $Gr_{x,C}$ (and N) may be negative. Thus the differences in transport are seen to be due to $\theta'(\xi,0)$, $\phi'(\xi,0)$, and N. For $Le = 1$, the differences are entirely due to N. It may further be noted that the present problem for Darcy flow with an impermeable cylindrical surface had been investigated by Yücel [12]. For the same flow, with $\xi = 0$, the above equations reduce to those for natural convection about a flat plate. Hence, deviation from $\xi = 0$ measures the effect of transverse curvature. It should be noted that as $r_0 \to \infty$, or for thin boundary layers where r does not differ appreciably from r_0, the pseudo-similarity variable η reduces to the corresponding similarity variable for a flat plate. However, the similarity treatment as well as an integral treatment of the natural convection Darcy flow with conjugate heat and mass transfer effects for a flat plate case has recently been investigated by Nakayama and Hossain [14].

3. METHODS OF SOLUTION

In the present analysis, it is proposed to investigate the problem posed by the coupled nonsimilarity equations (15–17) by employing the implicit finite difference method with Keller-box elimination method and the local nonsimilarity method.

3.1. Finite-difference method (FDM)

To implement this method, the coupled partial differential equations (15–17) are first reduced to a set of ordinary differential equations by replacing the partial derivatives with respect to η by a finite-difference formula centered at (ξ, η)-interval midpoint. The resulting set of ordinary differential equations are in turn reduced to a nonlinear system of algebraic equations which are then linearized by using Newton's quasi-linearization technique. Finally, the Keller-box elimination method has been introduced to get the corrections to the involved functions. Details of the

method have already been discussed in Hossain and Nakayama [20]. To initiate the solution, the profiles for the functions and their derivatives $\xi = 0$ for different values of pertinent parameters are used from the exact solutions of the equations (24–26) at $\xi = 0$. The overall computations were carried out on a DX-II personal computer, considering variable grids in the η-direction, defined by $\eta_j = \sinh(\eta_j/a)$. With $a = 100$, j is allowed to vary automatically so that η_∞ belongs to the interval $10 < \eta_\infty < 20$; this gives rise to convergent solutions with the desired accuracy for given values of the pertinent parameters. In order to assess the accuracy of this method, we have compared the solutions obtained by local nonsimilarity method upto the third level of truncation as discussed below.

3.2. Local non-similarity method (LNS)

This section deals with the local non-similarity method initiated by Sparrow and Yu [23] and has since been applied by many investigators to solve various nonsimilarity boundary value problems. Formulation of the system of equations for the local nonsimilarity model with reference to the present problem will now be discussed.

At the first level of truncation, the terms accompanied by $\xi()/\partial\xi$ are small. This is particularly true when $\xi \ll 1$. Thus the terms with $\xi()/\partial\xi$ on the right hand sides of equations (15)–(17) are deleted to get the following system of equations:

$$f'' + 2\,Gr^*\,(1+N)\,f'f'' = \frac{\theta' + N\phi'}{1+N} \tag{24}$$

$$(1+\xi\,\eta)\,\theta'' + \frac{1}{2}\,(f+2\,\xi)\,\theta' = 0 \tag{25}$$

$$\frac{1}{Le}\,(1+\xi\,\eta)\,\phi'' + \frac{1}{2}\,(f+2\,\xi)\,\phi' = 0 \tag{26}$$

equations (24–26) can be regarded as a system of ordinary differential equations for the functions f, θ and ϕ, with ξ as a parameter for given pertinent parameters. For the higher level of truncations, we introduce the following functions:

$$f_1 = \frac{\partial f}{\partial \xi},\quad \theta_1 = \frac{\partial \theta}{\partial \xi},\quad \phi_1 = \frac{\partial \phi}{\partial \xi}$$

$$f_2 = \frac{\partial f_1}{\partial \xi},\quad \theta_2 = \frac{\partial \theta_1}{\partial \xi},\quad \phi_2 = \frac{\partial \phi_1}{\partial \xi} \tag{27}$$

and obtain the equations upto the third level of truncations. Thus, the equations up to the third level of truncations obtained are as follows:

$$f'' + 2\,Gr^*\,(1+N)\,f'\,f'' = \frac{\theta' + N\,\phi'}{1+N} \tag{28}$$

$$(1+\xi\,\eta)\,\theta'' + \frac{1}{2}\,(f+2\,\xi)\,\theta' = \frac{1}{2}\,\xi\,(f'\,\theta_1 - \theta'\,f_1) \tag{29}$$

$$\frac{1}{Le}\,(1+\xi\,\eta)\,\phi'' + \frac{1}{2}\,(f+2\,\xi)\,\phi' = \frac{1}{2}\,\xi\,(f'\phi_1 - \phi' f_1) \tag{30}$$

$$f_1'' + 2\,Gr^*\,(1+N)\,(f'\,f_1'' + f''\,f_1') = \frac{\theta_1' + N\,\phi_1'}{1+N} \tag{31}$$

$$(1+\xi\,\eta)\,\theta_1'' + \frac{1}{2}\,(f+2\xi)\,\theta_1' + f_1\,\theta' - \frac{1}{2}\,f'\,\theta_1 + \eta\,\theta'' + \theta'$$

$$= \frac{1}{2}\,\xi\,(f'\,\theta_2 + f_1'\,\theta_1 - \theta'\,f_2 - f_1\,\theta_1') \tag{32}$$

$$\frac{1}{Le}\,(1+\xi\,\eta)\,\phi_1'' + \frac{1}{2}\,(f+2\,\xi)\,\phi_1' + f_1\,\phi' - \frac{1}{2}\,f'\,\phi_1 + \eta\,\phi'' + \phi'$$

$$= \frac{1}{2}\,\xi\,(f'\,\phi_2 + f_1'\,\phi_1 - \phi'\,f_2 - f_1\,\phi_1') \tag{33}$$

$$f_2'' + 2\,Gr^*\,(1+N)\,(f'\,f_2'' + 2\,f_1'\,f_1'' + f''\,f_2')$$

$$= \frac{\theta_1' + N\,\phi_1'}{1+N} \tag{34}$$

$$(1+\xi\,\eta)\,\theta_2'' + \frac{1}{2}\,(f+2\,\xi)\,\theta_2' + \frac{3}{4}\,f_2\,\theta' - f_1'\,\theta_1 + 2\,f_1\,\theta'$$

$$+2\,\theta_1' + 2\,\eta\,\theta_1''$$

$$= \frac{1}{2}\,\xi\,(2\,f'\,\theta_2 + f_2'\,\theta_1 - 2\,\theta'\,f_2 - f_1\,\theta_2') \tag{35}$$

$$\frac{1}{Le}\,(1+\xi\,\eta)\,\phi_2'' + \frac{1}{2}\,(f+2\,\xi)\,\phi_2' + \frac{3}{4}\,f_2\,\phi' - f_1'\,\phi_1$$

$$+2\,f_1\,\theta' + 2\,\phi_1' + 2\,\eta\,\phi_1''$$

$$= \frac{1}{2}\,\xi\,(2\,f'\,\phi_2 + f_2'\,\phi_1 - \phi_2'\,f_1 - 2\,f_2\,\phi_1') \tag{36}$$

The set of equation (31–33) is obtained by differentiating the set of equation (28–30) with respect to ξ. In this set, all the terms on the right hand side are retained. Again, equations (31–33) are differentiated with respect to ξ to get the set of equations (34–36). In this set, the ξ-derivatives of the functions f_2, θ_2 and ϕ_2 are neglected. The boundary conditions to be satisfied by the above sets of equations are:

$$\left.\begin{aligned} f = f_w,\ \theta = 1,\ \phi = 1 \ \text{ at } \ \eta = 0 \\ f' = 0,\ \theta = 0,\ \phi = 0 \ \text{ as } \ \eta \to \infty \end{aligned}\right\} \tag{37}$$

$$\left.\begin{aligned} f_1 = 0,\ \theta_1 = \phi_1 = 0 \ \text{ at } \ \eta = 0 \\ f_1' = \theta_1 = \phi_1 = 0 \ \text{ as } \ \eta \to \infty \end{aligned}\right\} \tag{38}$$

TABLE I
Numerical values of local Nusselt number and Sherwood number for different values of f_w.

	$Nu_x\ Ra_{x,t}^{-1/2}$				$Sh_x\ Ra_{x,c}^{-1/2}$			
ξ	FDM	LNS	DM	LNS	FDM	LNS	FDM	LNS
	$f_w = 1.0$		$f_w = -1.0$		$f_w = 1.0$		$f_w = -1.0$	
0.0	0.4253	0.4256	0.4253	0.4256	0.6015	0.6020	0.6015	0.6020
0.4	0.3356	0.3280	0.7672	0.7879	0.4746	0.4639	1.0850	1.1143
0.8	0.2749	0.2701	1.1671	1.2065	0.3887	0.3819	1.6506	1.7063
1.0	0.2523	0.2345	1.3809	1.4290	0.3569	0.3316	1.9529	2.0209
2.0	0.1818	0.2113	2.5303	2.5994	0.2570	0.2988	3.5784	3.6761
3.0	0.1464	0.1954	3.7353	3.8049	0.2071	0.2764	5.2826	5.3809
4.0	0.1265	0.1606	4.9526	5.0201	0.1789	0.2272	7.0040	7.0995
5.0	0.1143	0.1529	6.1730	6.2382	0.1617	0.2162	8.7300	8.8222
6.0	0.1064	0.1470	7.3948	7.4575	0.1505	0.2079	10.457	10.546
7.0	0.1010	0.1437	8.6173	8.6771	0.1428	0.2033	12.186	12.271
8.0	0.0971	0.1416	9.8401	9.8964	0.1373	0.2003	13.916	13.995
9.0	0.0942	0.1386	11.0633	11.0847	0.1332	0.1961	15.645	15.676
10.0	0.0919	0.1377	12.2867	12.2720	0.1300	0.1947	17.376	17.355

$$\left.\begin{aligned} f_2 = \theta_2 = \phi_2 = 0 \ \text{ at } \ \eta = 0 \\ f_2' = \theta_2 = \phi_2 = 0 \ \text{ as } \ \eta \to \infty \end{aligned}\right\} \tag{39}$$

As at the lower levels, the system of equations, equations (28)–(36) together with the boundary conditions (37)–(39), contains nine functions $f, f_1, f_2, \theta, \theta_1, \theta_2, \phi, \phi_1$, and ϕ_2 that are mutually coupled. The total order of this system is now 18. For given values of the pertinent parameters, these equations can again be treated as ordinary differential equations that contain the parameter ξ. From the solutions of the above equations, we are interested in obtaining solutions only for the functions f, θ, and ϕ and their derivatives. The above system of 9 equations is solved using the implicit Runge–Kutta method in conjunction with the Nachtsheim–Swigert iteration technique. The details of the computational technique have already been discussed in Hossain and Nakayama [20] and Hossain et al. [24]. It should be noted here that in getting the convergence of the solutions, the maximum number of iterations was 5–7 to satisfy the required tolerance of the convergence, which was taken 10^{-6}.

4. RESULTS AND DISCUSSIONS

In the present investigation, results are obtained by two distinct methodologies, namely, the implicit finite-difference method with Keller-box scheme and the local nonsimilarity method with third order level of truncation. Numerical values are obtained in terms of local Nusselt number Nu_x and local Sherwood number Sh_x for different values of the pertinent parameters. These parameters are the modified Grashof number Gr^*, buoyancy parameter N, Lewis number Le, and the curvature parameter $\xi\,(0 \leqslant \xi \leqslant 10)$ for the flow along a permeable cylindrical surface in a porous medium. Effects of these parameters on the velocity, temperature and the species concentration profiles are also shown graphically. The numerical values of the local Nusselt number and the local Sherwood number obtained by the two methods mentioned above are tabulated in *table I* for the pertinent parameters values $Gr^* = 1.0$, $N = 1.0$, $Le = 1.0$, and $f_w = 1.0$ and -1.0. The comparison between the numerical values obtained by the above two methods shows an excellent agreement between them for both local Nusselt and Sherwood numbers. It is also noticed from this table that the values of both Nu_x, and Sh_x, decrease with the increase of the curvature parameter while fluid is injected through the permeable surface of the cylinder. On the other hand, values of these physical quantities increase with increasing curvature effect when fluid is being sucked through the permeable surface. This is due to the effect of both thermal and concentration boundary layer thicknesses on the physical quantities. For the case of fluid injection, the boundary layer thickness becomes thicker with increasing the curvature parameter and as

a result the Nusselt and Sherwood numbers decrease. *Table II* represents the numerical values of the local Nusselt number, Nu_x, and the Sherwood number, Sh_x, for the case of impermeable cylindrical surface with parameter values $Gr^* = 1.0$, 10.0 and 100.0, $N = 5.0$, and $Le = 10.0$. The values of the curvature parameter are chosen as in the previous case. These results are solely obtained by using the implicit finite-difference method. From *table II* one can see that the numerical values of both Nu_x and Sh_x decrease due to an increase in the value of the Grashof number, Gr^*. As the modified Grashof number increases, the drag forces created by the solid matrix increases and as a result the temperature and the concentartion gradients decrease. Moreover, an increase in the curvature effect leads to an increase in the values of these physical quantities at the surface. Therefore, the effect of the transverse curvature (ξ) is to sharpen the variations near the surface. In *table III*, numerical values of the local Sherwood number for different values of the Lewis number Le (= 1, 10, 50 and 100.0) with $Gr^* = 10.0$, $N = 1.0$ and $f_w = 0.0$. Since the effect of the Lewis number on the local Nusselt number is not found to be significant, the results are not shown in this table. However, from this table, one can observe that the Lewis number has a significant effect on the values of the Sherwood number. As the Lewis number increases, the Sherwood number increases. This is because the concentration boundary layer becomes increasingly thinner as Le increases. A similar effect of this parameter on the Lewis number had been observed in case of the flow along a flat plate [14].

TABLE II
Numerical values of local Nusselt number and Sherwood number for different values of Gr^* when $N = 5.0$, $Le = 10.0$, and $f_w = 0.0$.

	$Nu\ Ra_{x,t}^{-1/2}$			$Sh\ Ra_{x,c}^{-1/2}$		
ξ/Gr^*	1.0	10.0	100.0	1.0	10.0	100.0
0.0	0.5066	0.3356	0.2274	0.9886	0.6049	0.3490
0.2	0.6124	0.4654	0.3865	1.0339	0.6503	0.3934
0.4	0.7208	0.5910	0.5239	1.0779	0.6939	0.4355
0.6	0.8291	0.7109	0.6502	1.1209	0.7360	0.4763
0.8	0.9360	0.8259	0.7694	1.1629	0.7768	0.5161
1.0	1.0411	0.9368	0.8834	1.2041	0.8166	0.5555
2.0	1.5406	1.4509	1.4067	1.4000	1.0044	0.7486
3.0	2.0063	1.9238	1.8848	1.5834	1.1808	0.9390
4.0	2.4495	2.3720	2.3366	1.7579	1.3513	1.1267
5.0	2.8764	2.8028	2.7703	1.9259	1.5185	1.3113
6.0	3.2910	3.2207	3.1903	2.0891	1.6837	1.4926
7.0	3.6955	3.6281	3.5995	2.2486	1.8475	1.6708
8.0	4.0918	4.0269	3.9999	2.4052	2.0103	1.8461
9.0	4.4810	4.4184	4.3927	2.5595	2.1721	2.0188
10.0	4.8642	4.8036	4.7790	2.7119	2.3330	2.1891

TABLE III
Numerical values of Sh_x against ξ for different values of Le with $N = 1.0$ and $f_w = 0$ obtained by finite difference method.

ξ/Le	1.0	10.0	50.0	100.0
0.0	0.4722	1.6181	3.6774	5.2180
0.4	0.5897	1.7325	3.7942	5.3354
0.8	0.7061	1.8415	3.9084	5.4508
1.2	0.8221	1.9462	4.0204	5.5646
2.0	1.0519	2.1458	4.2391	5.7885
4.0	1.6050	2.6050	4.7606	6.3291
6.0	2.1278	3.0319	5.2534	6.8464
8.0	2.6274	3.4440	5.7232	7.3440
10.0	3.1093	3.8495	6.1741	7.8247

The effect of the modified Grashof number and the curvature parameter on the velocity, temperature, and the species concentration profiles is shown in *figure 2* with $N = 5.0$, $Le = 10.0$, and $f_w = 0.0$. It is observed from this figure that an increase in the value of the Grashof number leads to a decrease in the velocity peak, which occurs at the surface. This happens because the inertia term begins to have a pronounced effect for high Grashof numbers. Moreover, for a fixed value of Grashof number, an increase in the transverse curvature results in a decreasing of the velocity profiles. From this figure we further observe that the temperature and the concentration distributions in the boundary layer increase owing to increase in the value of the Grashof number and as a result both the thermal and velocity boundary layers become thicker. Finally, the effect of the Lewis number and the transpiration parameter on the velocity, temperature, and the species distributions are shown in *figure 3* for $\xi = 2.5$ with $N = 5.0$ and $Gr^* = 10.0$. In this figure the solid, dotted, and broken curves represent the distributions for $f_w = -1.0$, 0.0 and 1.0, respectively. It is observed from this figure that the suction of fluid through the surface of the cylinder leads to an increase in the velocity, temperature, and the concentration profiles while blowing of fluid leads to a decrease in the velocity, the temperature as well as the species concentration distributions in the boundary layer regime. We further observe that the velocity, the temperature and the concentration distribution decrease due to an increase in the value of the Lewis number. As mentioned earlier, increasing Le is to thicken the temperature boundary layer and to thin the concentration boundary layer.

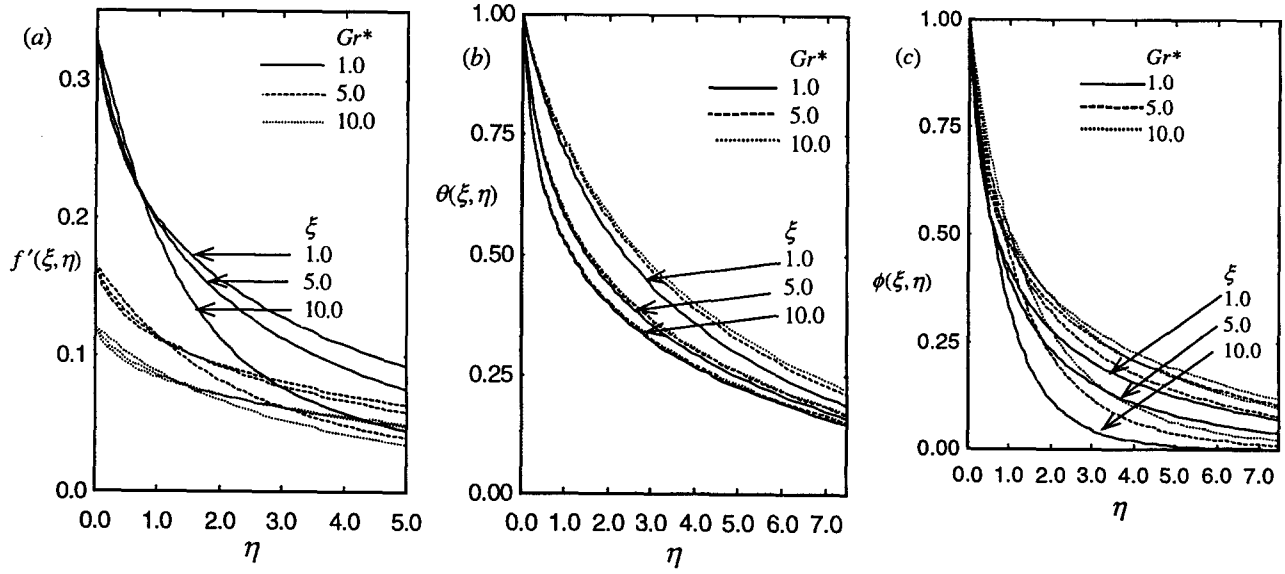

Figure 2. Velocity (a), temperature (b) and species concentration profiles (c) against η for different Gr^* and ξ with $Le = 10.0$, $N = 5.0$ and $f_w = 0.0$.

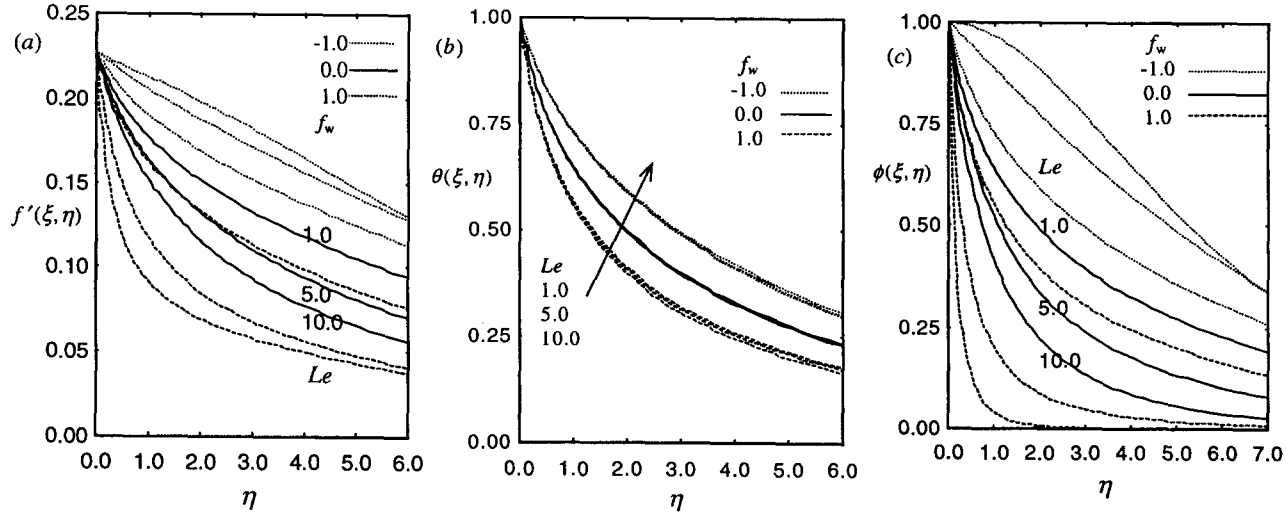

Figure 3. Velocity (a), temperature(b) and species concentration profiles (c) against η for different Le and f_w with $Gr^* = 10.0$, $N = 5.0$ and $\xi = 2.5$.

5. CONCLUSIONS

Extensive numerical integrations were carried out, using the implicit finite difference technique together with the Keller-box method and the local nonsimilarity method, to investigate the non-Darcy natural convection heat and mass transfer from a vertical cylinder with surface mass flux. The numerical values are furnished for wide ranges of the parameters associated with the porous inertia, transverse radial curvature, surface mass flux and the combined buoyancy parameter. The individual and combined effect of these parameters on the velocity field, the temperature field and the concentration field are elucidated and presented graphically. The results obtained by two methods are compared in tabular form and found to be in excellent agreement. From the present analysis we may conclude that (1) both the local Nusselt number, Nu_x, and the Sherwood number, Sh_x, decrease with the increase of the curvature parameter while fluid is injected through the permeable surface of the cylinder. On the other hand, values of these physical quantities increase with increasing curvature effect when fluid is being sucked

through the permeable surface and (2) both Nu_x and Sh_x decrease due to increase in the value of the Grashof number, Gr^*.

REFERENCES

[1] Cheng P., Geothermal heat transfer, in: Rohsenow W.M. et al. (Eds.), Handbook of Heat Transfer Application, 2nd Ed., Chap 11., McGraw-Hill, New York, 1985.

[2] Kulacki F.A., Keyhani M., in: McAssey E.V. Jr., Schrock V.E. (Eds.), Heat transfer aspects of nuclear waste disposal, HTD, vol. 67, ASME, New York, 1987, pp. 1–17.

[3] Neild D.A., Onset of thermohaline convection in a porous medium, Water Resour. Res. 4 (1968) 553–560.

[4] Gershuni G.Z., Zukhovitaski E.M., Lyubimov D.Y., Thermal concentration instability of a mixture in a porous medium, Sov. Phys. Dokl. 21 (1976) 375–377.

[5] Yang J.Y., Chang W.J., The flow and vortex instability of horizontal natural convection in a porous medium resulting from combined heat and mass buoyancy effects, Int. J. Heat Mass Tran. 31 (1988) 769–777

[6] Pera L., Gebhart B., On the stability of natural convection boundary layer flow over horizontal and slightly inclined surface, Int. J. Heat Mass Tran. 16 (1973) 1147–1163.

[7] Chen T.S., Tzuoo K.L., Moutsoglou A., Vortex instability of horizontal and inclined natural convection flows from simultaneous thermal and mass diffusion, J. Heat Trans.–T. ASME 105 (1983) 774–781.

[8] Bejan A., Khair K.R., Heat and mass transfer by natural convection in porous medium, Int. J. Heat Mass Tran. 28 (1985) 909–918.

[9] Trevisan O.V., Bejan A., Natural convection with combined heat and mass transfer buoyancy effects in a porous medium, Int. J. Heat Mass Tran. 28 (1985) 1597–1611.

[10] Rapits A., Tzivanidis G., Kafousias N., Free convection and mass transfer flow through a porous medium bounded by an infinite vertical limiting surface with constant suction, Lett. Heat Mass Tran. 8 (1981) 417–424.

[11] Evans D.G., Nunn J.A., Free thermoheline convection in sediments surrounding a salt column, J. Geophys. Res. 94 (1989) 12413–1242.

[12] Yücel A., Natural convection heat and mass transfer along a vertical cylinder in porous medium, Int J. Heat Mass Tran. 33 (1990) 2265–2274.

[13] Bejan A., Convective Heat Transfer, Chap. 1, Wiley, New York, 1984, pp. 335–338.

[14] Nakayama A., Hossain M.A., An integral treatment for combined heat and mass transfer by natural convection in a porous medium, Int. J. Heat Mass Tran. 38 (1995) 761–765.

[15] Vafai K., Tien C.L., Boundary and inertia effects on flow and heat transfer in porous media, Int. J. Heat Mass Tran. 24 (1981) 195–203.

[16] Vafai K., Whitaker S., Simultaneous heat and mass transfer accompanied by phase change in porous insulation, J. Heat Trans.–T. ASME 108 (1986) 132–140.

[17] Minkowycz W.J., Cheng P., Free convection about a vertical cylinder embedded in a porous medium, Int. J. Heat Mass Tran. 19 (1976) 805–813.

[18] Vasanth R., Pop I., Nath G., Non-Darcy natural convection over a slender vertical frustum of a cone in a saturated porous medium, Int. J. Heat Mass Tran. 29 (1986) 153–156.

[19] Ingham D.B., The non-Darcy free convection boundary layer on axi-symmetric and two-dimensional bodies of arbitrary shape, Int. J. Heat Mass Tran. 29 (1986) 1759–1763.

[20] Hossain M.A., Nakayama A., Non-Darcy free convection flow along a vertical cylinder embedded in a porous medium with surface mass flux, Int. J. Heat Fluid Fl. 14 (1993) 385–390.

[21] Fard M.K., Charrier-Mojtabi M.C., Vafai K., Non-Darcian effects on double diffussive convection within a porous medium, Numer. Heat Tr. 31 (1997) 837–852.

[22] Plumb O.A., Huenefeld J.C., Non-Darcy natural convection from heated surfaces in saturated porous medium, Int J. Heat Mass Tran. 24 (1981) 765–768.

[23] Sparrow E.M., Yu H.S., Local nonsimilarity thermal boundary-layer solutions, J. Heat Trans.-T. ASME 93 (1971) 328–332.

[24] Hossain M.A., Banu N., Nakayama A., Non-Darcy forced convection flow over a wedge embedded in a porous medium, Numer. Heat Tr. A 26 (1994) 399–414.

❑